Dilution effects on ultrafine particle emissions from Euro 5 and Euro 6 diesel and gasoline vehicles

Cédric Louis, Yao Liu, Simon Martinet, B d'Anna, Alvaro Martinez Valiente, Antoinette Boreave, Badr R'Mili, Patrick Tassel, Pascal Perret, Michel Andre

Accepted Manuscript

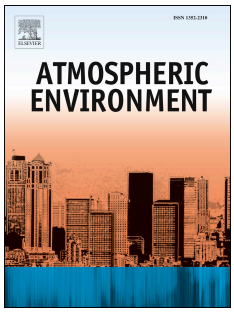

Dilution effects on ultrafine particle emissions from Euro 5 and Euro 6 diesel and gasoline vehicles

Cédric Louis, Yao Liu, Simon Martinet, Barbara D'Anna, Alvaro Martinez Valiente, Antoinette Boreave, Badr R'Mili, Patrick Tassel, Pascal Perret, Michel André

PII: S1352-2310(17)30589-7

DOI: 10.1016/j.atmosenv.2017.09.007

Reference: AEA 15545

To appear in: *Atmospheric Environment*

Received Date: 8 March 2017

Revised Date: 22 August 2017

Accepted Date: 3 September 2017

Please cite this article as: Louis, Cé., Liu, Y., Martinet, S., D'Anna, B., Valiente, A.M., Boreave, A., R'Mili, B., Tassel, P., Perret, P., André, M., Dilution effects on ultrafine particle emissions from Euro 5 and Euro 6 diesel and gasoline vehicles, *Atmospheric Environment* (2017), doi: 10.1016/j.atmosenv.2017.09.007.

Dilution effects on ultrafine particle emissions from Euro 5 and Euro 6 diesel and gasoline vehicles

Cédric Louis [a,b], Yao Liu [a,*], Simon Martinet [a], Barbara D'Anna [c], Alvaro Martinez Valiente [c], Antoinette Boreave [c], Badr R'Mili [c], Patrick Tassel [a], Pascal Perret [a], Michel André [a]

[a] Univ Lyon, IFSTTAR, AME, LTE, F-69675, LYON, France
[b] French Environment and Energy Management Agency, ADEME, 49004 Angers, France
[c] IRCELYON – UMR 5256 CNRS – Université de Lyon, 69626 Villeurbanne, France
* Corresponding author: yao.liu@ifsttar.fr, 25 avenue François Mitterrand, 69675 Bron, France

Abstract

Dilution and temperature used during sampling of vehicle exhaust can modify particle number concentration and size distribution. Two experiments were performed on a chassis dynamometer to assess exhaust dilution and temperature on particle number and particle size distribution for Euro 5 and Euro 6 vehicles. In the first experiment, the effects of dilution (ratio from 8 to 4000) and temperature (ranging from 50 °C to 150 °C) on particle quantification were investigated directly from tailpipe for a diesel and a gasoline Euro 5 vehicles. In the second experiment, particle emissions from Euro 6 diesel and gasoline vehicles directly sampled from the tailpipe were compared to the constant volume sampling (CVS) measurements under similar sampling conditions. Low primary dilutions (3–5) induced an increase in particle number concentration by a factor of 2 compared to high primary dilutions (12–20). Low dilution temperatures (50 °C) induced 1.4–3 times higher particle number concentration than high dilution temperatures (150 °C). For the Euro 6 gasoline vehicle with direct injection, constant volume sampling (CVS) particle number concentrations were higher than after the tailpipe by a factor of 6, 80 and 22 for Artemis urban, road and motorway, respectively. For the same vehicle, particle size distribution measured after the tailpipe was centred on 10 nm, and particles were smaller than the ones measured after CVS that was centred between 50 nm and 70 nm. The high particle concentration (≈10^6 #/cm^3) and the growth of diameter, measured in the CVS, highlighted aerosol transformations, such as nucleation, condensation and coagulation occurring in the sampling system and this might have biased the particle measurements.

Keywords

Gasoline and diesel emissions; CVS; Tailpipe; Dilution; Temperature; Ultrafine particle; Nucleation; Condensation; Coagulation

Abbreviations

G-DI	Gasoline with Direct Injection	DPF	Diesel Particulate Filter
cat	Catalysed Filter	PMP	Particle Measurement Programme
CVS	Constant Volume Sampler	FPS	Fine Particle Sampler
NO_X	Nitrogen Oxides	NO_2	Nitrogen Dioxide
NO	Nitric Oxide	PN	Particle Number
CPC	Condensation Particle Counter	ELPI	Electrical Low Pressure Impactor
SMPS	Scanning Mobility Particle Sizer	FMPS	Fast Mobility Particle Sizer Spectrometer
HEPA	high-efficiency particulate air		

1 Introduction

Vehicle exhaust emissions represent a major source of particle matter in urban environments. On regional and global scales, atmospheric particles play an important role in human health and climate change (Ning, 2010; Kulmala et al., 2000; Pope III, 2000). Particles emitted from diesel and gasoline engines are ultrafine particles with size ranges of 20–130 nm and 20–60 nm, respectively (Karjalainen et al., 2014; Morawska et al., 2008; Burtscher 2005; Jamriska et al., 2004). The ultrafine particles represent only 0.1–10% of the total particulate mass, but it might represent more than 90% of the total particle number (Giechaskiel et al., 2010; Kittelson, 1998). Particle emission depends on the engine technology, fuel and aftertreatment devices. Liang et al. (2013) and Köhler (2013) showed that the gasoline direct injection (G-DI) technology induced an increase in the particle number concentration compared to the standard gasoline passenger cars. Moreover, the dilution process (dilution ratio, dilution gas temperature and sampling residence time) has been established as a factor influencing ultrafine particle formation (Manoukian et al., 2016; Wei et al., 2016; Ranjan et al., 2012; Fujitani et al., 2012; Mamakos and Martini, 2011; Grieshop et al., 2009a; Vouitsis et al., 2008; Rönkkö et al., 2006; Mathis et al. 2004). After the tailpipe, the exhaust undergoes high and fast atmospheric dilution ratio that could reach up from 1000 to 4000 in 1–3 s (Fujitani et al., 2012; Zhang and Wexler, 2004). The exhaust temperature (around 200 °C) decreases rapidly at ambient temperature level within few seconds after emission due to the high dilution ratio. The rapid decrease in temperature has significant implications in terms of thermodynamics of particles and semi-volatile compounds (Kim et al., 2016; Huang et al., 2014; May et al., 2013; Wang and Zhang, 2012; Kozawa et al., 2012; Mamakos and Martini, 2011; Casati et al., 2007; Morawska et al., 2008; Zhang et al., 2004) leading to a drastic change in particle number concentration and size distribution (Huang et al., 2014; Wang and Zhang, 2012; Uhrner et al., 2011; Grieshop 2009b). Although several recent studies have focused on that issue, uncertainties still remain regarding the experimental determination of ultrafine particle emissions from vehicle exhaust and the impact of dilution and temperature during their sampling (Wei et al., 2016; Manoukian et al., 2016; Ranjan et al., 2012; Fujitani et al., 2012; Grieshop et al., 2009a).

Particle number concentration is measured through a specific protocol, derived from the Particle Measurement Program (PMP) through the full-flow Constant Volume Sampler (CVS). This protocol requires the removal of the volatile phase by the dilution stage (150 °C) and a heated tube (at 300–400 °C). The PMP approach only regulates the non-volatile fraction of particles in order to exclude the possible confounding of measurement data by low volatility hydrocarbons manifesting as a nucleation mode present below 20 nm that highly depends on the sampling conditions (Giechaskiel et al., 2008). In the atmosphere, the concentration of aerosols changes rapidly in the first seconds after emission with condensation phenomenon and presence of SVOCs, which strongly depend on the exhaust sampling (length of the sampling line, dilution factor, temperature, etc.) (Albriet et al., 2010). Several studies showed that the ultrafine particle number concentration directly measured from the tailpipe was significantly different than those from the CVS (Kim et al., 2016; Giechaskiel et al., 2010, 2007; Mathis et al., 2005). Giechaskiel et al. (2010) showed that deceleration (from 140 km/h to 120 km/h) induced a higher particle number concentration with higher mean diameter than acceleration (from 90 km/h to 120 km/h) with a Euro 3 diesel vehicle without particulate filter. This observation is in contrast with their previous work (Giechaskiel et al., 2007), which reported a lower particle number concentration during deceleration than during acceleration. This contradiction can be explained by differences in sampling systems. According to Giechaskiel et al. (2007), particles were sampled directly from the tailpipe, while in Giechaskiel et al. (2010), particles were sampled from the CVS. As mentioned by Giechaskiel et al. (2014), the CVS dilution tunnel has several disadvantages such as the inability to control the dilution ratio and the dilution temperature, a long sampling path and a long

residence time. This dilution system favours nucleation, condensation and coagulation that could induce the new particle formation or the modification of the particle size distribution.

Based on this evidence, the particle measurement directly from the tailpipe was considered as a complementary sampling method to CVS in order to understand the sampling condition impacts on particle number concentration. This work aimed to investigate the impacts of dilution and temperature on particle emissions after a CVS tunnel system and directly from the tailpipe with Euro 5 and Euro 6 vehicles. Particle number and size distribution between the CVS and the tailpipe were compared under similar dilution conditions to investigate the processes occurring in the dilution tunnel with the Euro 6 G-DI vehicle. Finally, we discussed the nucleation, condensation and coagulation phenomena observed into the CVS dilution system.

2 Materials and methods

2.1 Vehicle characteristics

Four currently in-use vehicles were studied: a Euro 5 gasoline with direct injection system (G-DI), and Euro 5 diesel with catalysed particulate filter (DPF cat), a Euro 6 G-DI and a Euro 6 DPF cat. Technical characteristics of the tested vehicles are shown in Table 1. All the tested vehicles were private vehicles to be as representative as possible of the state of the current French fleet. All experiments were conducted using commercial fuel (sulphur content less than 10 ppm) pumped from the same petrol station to minimize variability of fuel composition and its impact on emissions.

Table 1. Technical characteristics of the tested vehicles.

Vehicle	No. 1	No. 2	No. 3	No. 4
Size class	1.2	1.5	1.0	1.5
Technology	G-DI*	Diesel	G-DI*	Diesel
Standard	Euro5	Euro5	Euro 6	Euro 6
Empty weight (kg)	1320	1090	864	1087
Mileage (km)	25844	87073	2164	4700
Gearbox type	Manual (5)	Manual (5)	Manual (5)	Manual (5)
Registration date	27/02/2014	17/02/2012	11/12/2015	31/12/2015
Test date	31/03/2015	15/04/2015	29/03/2016	11/04/2016
Catalyst	Three-way	Oxidation	Three-way	Oxidation
Filter	No	Catalysed DPF[$]	No	Catalysed DPF[$]

* G-DI: Gasoline with direct injection system

[$] DPF: Diesel Particulate Filter

2.2 Experimental set-up

Emission measurements were performed on the chassis dynamometer at the Transports and Environment Laboratory (LTE) of the French Institute of Science and Technology for Transport, Development and Networks (IFSTTAR). The chassis dynamometer was composed of a 48-inch roller on which the drive wheels of the vehicle were placed. The dynamometer resisted to the vehicle rolling to simulate the road resistance, which was calculated based on road laws for each vehicle. The schema of the experimental setup is shown in Figure 1. Vehicle exhausts were sampled through two different ways: one directly at the tailpipe, diluted by the fine particle sampler (FPS) and the other through the CVS. Exhaust sampling from these two systems was diluted with filtered ambient air system.

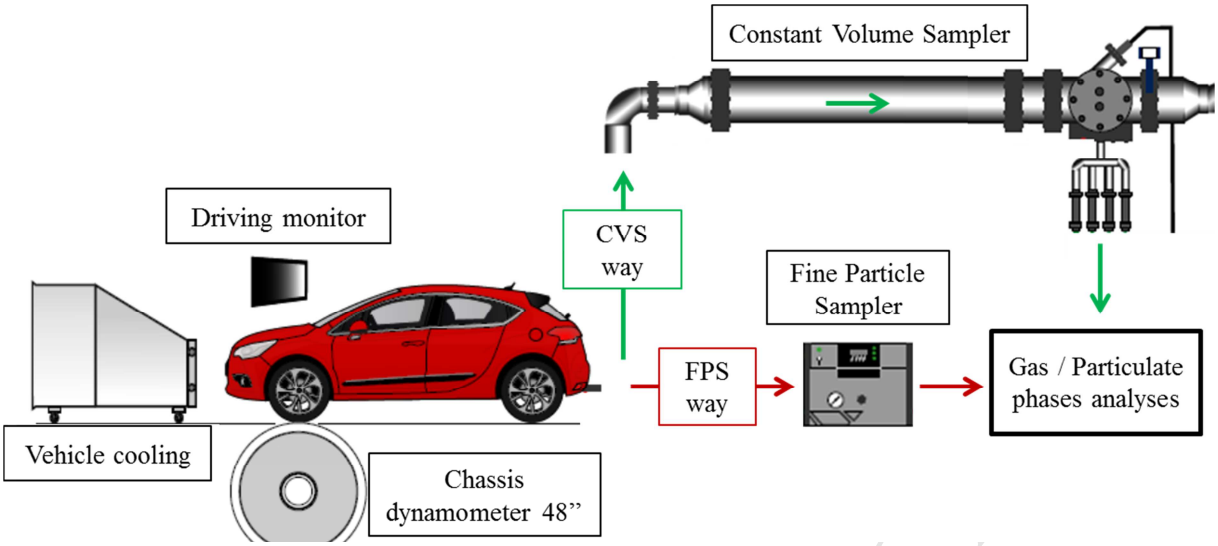

Figure 1. Schema of the experimental setup; the green arrows represent the CVS way and the red arrows represent the direct tailpipe way with FPS dilution.

2.2.1 Dilution systems

- Constant Volume Sampler (CVS)

Exhaust emissions measured using a CVS system were diluted with filtered ambient air (4 filters in series including M6-F7-F9, M5, F7 EN-779-2012 filters, a HEPA H13 EN1822-2009 filter and a cylindrical cartridge of charcoal scrubber). This filtered air allowed compensating the flow rate variations related to the exhaust flow fluctuations and keeping a constant volume sampling. The mixture air/exhaust went through the dilution tunnel, and then was monitored by different on-line gas and particulate phase analysers.

- Fine Particle Sampler (FPS)

A Fine Particle Sampler (FPS 4000, Dekati Ltd) was used for direct tailpipe dilution. The exhaust dilution was carried out in two stages: a primary dilution, close to the sampling point with controlled temperature and a secondary dilution as ejector type diluter, located downstream of the primary dilution and which adjusted the primary dilution to provide the total dilution. The FPS enabled the control of several dilution parameters such as sampling flow, primary dilution, total dilution and temperature.

2.2.2 Experimental protocol

Dilution and temperature effects were studied with two Euro 5 vehicles: gasoline (No. 1) and diesel (No. 2). The vehicles were tested with two Artemis cycles (motorway and urban) (André, 2004) and at 70 km/h steady speed. The particles were sampled from the tailpipe after the FPS dilution with or without VKL dilutors (depending on the total dilution tested). The FPS dilution temperatures were set at 50°C, 100°C, and 150°C and the total dilution ratios were 30, 100, 400, 1000, 2000 and 4000 for gasoline and 8, 12, 16, 30, 100, 400, 1000, 2000, 4000 for diesel. Each experimental condition was repeated three times.

To compare the tailpipe emissions with the CVS measurements, the Euro 6 gasoline (No.3) and the diesel (No.4) vehicles were tested with Artemis road, motorway and urban driving conditions. The detailed driving cycles with repeated tests and sampling conditions were shown in Table 2. The CVS operated at a total flow rate of 11 m^3/min for the Artemis motorway cycle and 9 m^3/min for the other driving cycles. The average CVS dilution ratios ranged between 13 and 60 for the gasoline vehicle and between 22 and 77 for the diesel vehicle, with a dilution temperature at 35 °C. At the

tailpipe the FPS primary dilution was set at 36°C to reproduce similar dilution and temperature conditions as in the CVS.

Table 2. Detailed driving cycles with test number and sampling conditions for the FPS and the CVS with Euro 6 G-DI (No.3) and Euro 6 diesel DPF cat (No.4) vehicles.

Vehicles	**Euro 6 G-DI (No. 3)**				**Euro 6 diesel DPF cat (No. 4)**			
Artemis cycles	Repeated number	CVS dilution	Total tailpipe dilution	Primary dilution	Repeated number	CVS dilution	Total tailpipe dilution	Primary dilution
Road	9	33	35	22	9	51	54	25
Urban	10	60	59	25	10	77	88	27
Motorway	6	13	15	12	6	22	18	17

2.3 Analytical methods

2.3.1 Regulated compound analysis

Regulated compounds, such as carbon oxide (CO), carbon dioxide (CO_2), total hydrocarbons (THC), nitric oxide (NO) and nitrogen oxides (NO_X) were monitored using a Horiba emission measurement system (CO and CO_2 by non-dispersive infrared, THC by flame ionization detection, NO and NO_X by chemiluminescence). The NO_2 concentration was determined by subtracting NO from NO_X. Regulated compounds were monitored to ensure that vehicles had regular emission behaviours with respect to their category and to detect any abnormalities that could introduce bias in the measurements.

2.3.2 Particulate phase analysis

The particle number concentration and the size distribution were measured by a Fast Mobility Particle Sizer Spectrometer (FMPS, model 3091 TSI). Particles went through a cyclone with a 1µm cut off and an electrical diffusion charger. The particle number concentration from 5.6 nm to 560 nm is determined by measuring the electrical current collected on a series of electrodes. Data were collected every second at 8 L/min. The quantification limit depended on the particle size: for 5.6 nm the maximum limit was 10^7 #/cm^3 and the minimum limit was 100 #/cm^3. Particle size number distribution was also characterised using an Electrical Low Pressure Impactor (ELPI, Dekati). The ELPI measured the particle number distribution in the 7 nm to 4 µm range with 12 filter stages. The operating flow rate of the ELPI was set at 10 L/min with a sampling period of 1s. The quantification limits ranged from 250 to 7×10^7 #/cm^3 for particles with a diameter between 7 nm and 4 µm and from 0.1 to 2×10^4 #/cm^3 for particles with a diameter greater than 4 µm. A Condensation Particle Counter (CPC, model 3775 TSI) was used for total particle number concentration. The CPC contained a butanol condensation chamber that enabled the detection of particles greater than 4 nm (particle size cut 50%). The operating flow rate of CPC was set at 1.5 L/min. The experimental data were collected every second with a concentration ranging from 0 to 10^7 #/cm^3.

The Particle Measurement Programme has been proposed as a regulatory approach for measuring particle numbers for Euro 5 and Euro 6 vehicles, with a 50% cut-point size of 23 nm. However, most particles emitted by the tested vehicles in our previous experiments were ultrafine particles with diameters below 23 nm, especially during the Artemis motorway driving cycle and

particulate filter regeneration (Louis et al., 2016). In order to have the most complete information on total particle number emissions including particles smaller than 23 nm, and to compare it with direct tailpipe emission, we did not fully follow the PMP protocol in this study. However the CVS tunnel was conditioned according the latest regulatory requirement in Europe with heated air dilution at 35°C. Furthermore, by considering the volatile fraction of particles, the standard variations of particle number concentration with six repeated tests, ranged from 7 to 11%.

3 Results and discussion

3.1 Dilution and temperature effects

For the Euro 5 gasoline vehicle, the exhaust was sampled directly from the tailpipe at different total dilution ratios through the FPS (at 30, 100, 400, 1000, 2000 and 4000). The total dilution ratios at 30, 400, 2000 and 4000 were obtained with low primary dilution ratios between 3 and 5, while the total dilution at 100 and 1000 were obtained with high primary dilution ratios between 12 and 20. Figure 2a showed the particle number concentration with the total dilution ratios between 30 and 4000 as function of the dilution temperature at 50, 100 and 150 °C during motorway driving condition. We observed that the temperature played an important role on particle concentrations. According to Beckers et al. (2009), low temperature (50 °C) induced 1.4 to 3 times more PN than high temperature (150 °C) for all tested dilution ratios. The PN concentrations were classified into two groups: black dots for total dilution of 30, 400, 2000 and 4000 characterized by a low primary dilution (3–5); white empty dots for the total dilution at 100, 1000 with high primary dilution (12–20). These latter total dilutions induced less particle emissions than dilution at 30, 400, 2000 and 4000 (Figure 2a). This can be explained by the fact that dilution ratios 100 and 1000 were achieved using high primary dilution ratio and it emphasised the key role of the primary dilution ratio. Figure 2b showed the particle number emissions from a gasoline vehicle as function of the primary dilution (3–20) under motorway driving condition with three primary dilution temperatures (50, 100 and 150°C). The particle number concentration was corrected taking into account the dilution factors. At low primary dilution (3–5) with the three tested dilution temperatures, PN concentrations were at $2–3\times10^{7}$ #/cm^{3}. For these sampling conditions, PN concentration did not depend on the dilution gas temperature. At high primary dilution conditions (12–20), PN concentration decreased with the increase in temperature. PN emissions were about 2 times lower (at $1–1.5\times10^{7}$ #/cm^{3}) at 100°C and 150°C than at 50°C. For the same temperature at 100 and 150 °C, the PN concentration decreased with the increase in the primary dilution ratio. These results were in agreement with the ones reported by Casati et al. (2007) for Euro3 diesel passenger cars. Their results indicated that the low primary dilution and the low dilution temperature of gas might promote the measurement bias. They recommended setting the sampling system at a high primary dilution and high dilution temperature to minimise those bias. For the Euro 5 diesel vehicle, PN emissions were low due to the high filtration efficiency of the diesel particulate filter (DPF). The particle number concentrations were lower than the detection limit of the instrument for most of the dilution conditions and were not presented.

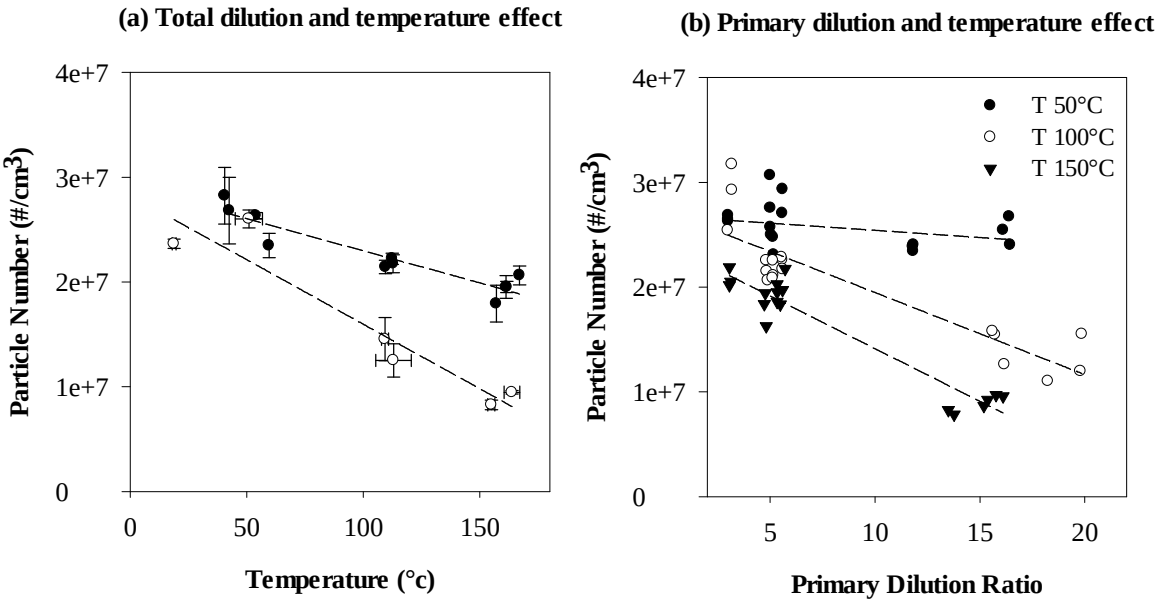

Figure 2. Total dilution and temperature effects (a) and primary dilution and temperature effects (b) for the gasoline Euro 5 vehicle (No. 1) during the motorway driving conditions, at 50°C, 100°C and 150°C. The particle number emissions are corrected taking into account of the dilution factors. For the figure 2a, the black dots show total dilution ratios at 30, 400, 2000 and 4000 with low primary dilution (3–5) and the white dots show total dilution ratios at 100 and 1000 with high primary dilution (12–20).

3.2 Euro 6 G-DI particle characterisation tailpipe / CVS

PN emissions measured from the tailpipe have also been compared with CVS measurements for two Euro 5 vehicles under Artemis motorway cycle. Statistically significant differences in PN concentration have been observed between these two sampling systems. Particle size distribution was unimodal and centred at 20 nm after the tailpipe (FPS sampling system) and at more than 60 nm after the CVS. However, different analysers have been used for the PN quantification at the tailpipe (with an ELPI) and after the CVS (with a SMPS) due to experimental organisation and constraints. Therefore, in order to better understand the physical processes occurring in the sampling systems, with their impact on PN measurement, two Euro 6 gasoline and diesel vehicles have been tested. The PN concentrations have been followed by a FMPS after the tailpipe and after the CVS with Artemis Urban, Road and Motorway cycles. Primary dilution at 20 was chosen to the tailpipe dilution in order to minimise the PN concentration measurement bias.

3.2.1 Particle concentration comparison between tailpipe and CVS

Due to the high efficiency of the diesel particulate filter, PN emission from the Euro 6 diesel vehicle was lower than the analyser detection limit. Therefore, only gasoline emissions were presented and discussed here. Table 3 showed the average particle number concentrations for Euro 6 gasoline G-DI for the Artemis urban, road and motorway driving cycles. The concentrations reported were average values of several repeated cycles for each driving condition. The PN measurement after CVS and tailpipe were performed under similar total dilution and temperature conditions (Table 2). PN concentrations from CVS were higher than at tailpipe by a factor of 6, 80 and 22 for Artemis urban, road and motorway, respectively. Highest discrepancies were observed under Artemis road cycle. Unfortunately, we did not find an explication, since the tests were repeated 5 and 3 times after CVS and exhaust, respectively, which showed similar result.

Table 3. Average particle number concentration for G-DI Euro 6 vehicle.

Particle concentration (#/cm^3) G-DI Euro 6						
Driving cycle		**Start**	**CVS**	**Tests Number**	**Exhaust**	**Tests Number**
Artemis	urban	hot start	(9 ± 5) x10^4	7	(1.4 ± 0.6) x10^4	3
Artemis	road	hot start	(2.3 ± 0.4) x10^6	5	(3 ± 2) x10^4	3
Artemis	motorway	hot start	(2.2 ± 0.1) x10^7	3	(1.0 ± 0.3) x10^6	3

3.2.2 Particle size distribution comparison between the tailpipe and the CVS

Figure 3 showed the particle number concentration and size distribution as a function of cycle time for the Euro 6 G-DI vehicle during an Artemis motorway driving cycle after the tailpipe (Figure 3a) and after the CVS (Figure 3b). At the tailpipe, particle emissions were characterised by narrow peaks of about 5s mainly during accelerations (Figure 3a), while after CVS particle emissions were characterised by larger emission peaks of about 30s and were observed for the whole cycle length (Figure 3b). Particle size distribution after tailpipe varied between 2 nm and 70 nm with a main mode at 10 nm. After the CVS the particle size distribution was centred at 50 nm and no particles below 30 nm were detected. This observation indicated that condensation and possibly coagulation happened. We observed an increase in PN after the CVS suggesting that also nucleation occurred in the CVS tunnel.

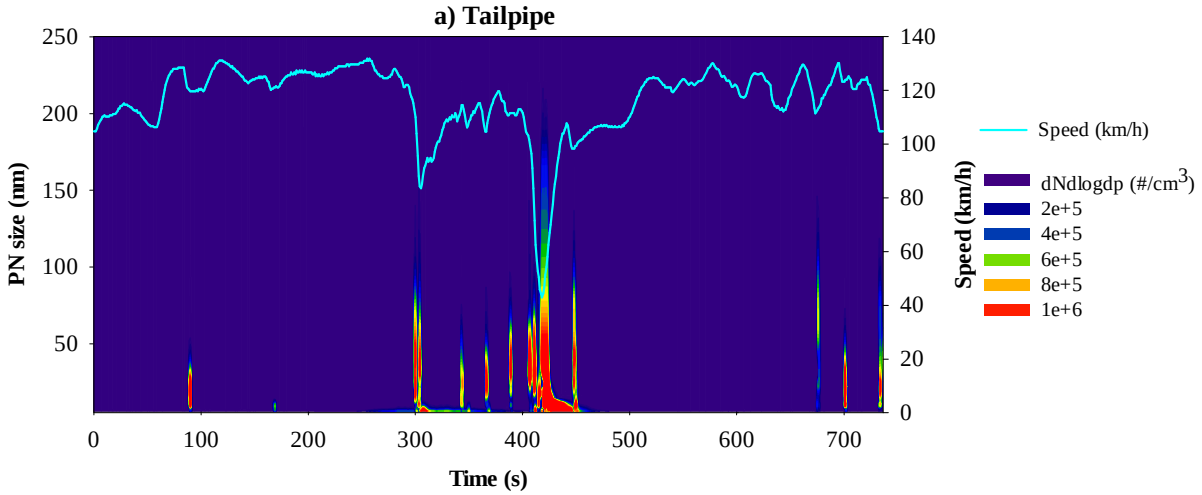

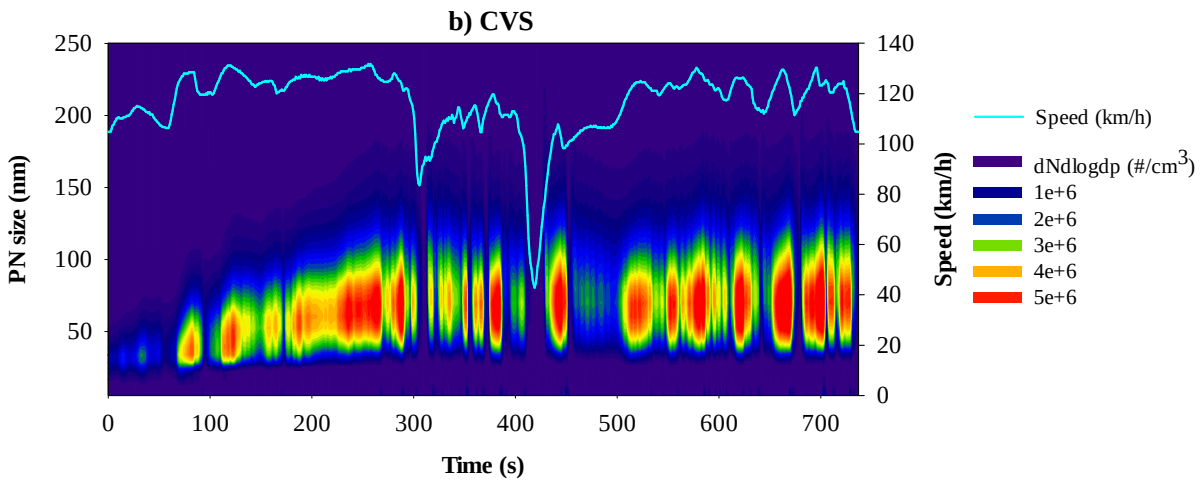

Figure 3. Particle number concentration of the G-DI vehicle during an Artemis motorway driving cycle, sampled: a) after the tailpipe and b) after the CVS. PN size distribution is described on the left Y-axis. The light blue line represents the vehicle speed (km/h) on the right Y-axis.

Vehicle accelerations lead to distinct emission peaks. An average of emissions over the whole cycle did not account for these disparities. In order to compare the CVS and exhaust particle size in an acceleration phase (high emission), we choose the highest emission peak for each cycle. Comparisons were made at 500s, 750s and 430s, respectively, for Artemis urban, road and motorway cycles. Figure 4 showed the PN size distribution for these three driving conditions after the tailpipe (Figure 4a) and after the CVS (Figure 4b). For motorway, both tailpipe and CVS particle size distribution were unimodal. However, the CVS measurement showed a higher PN concentration with the particle diameter centred at 70 nm comparing to the tailpipe, for which the particle diameter was smaller and centred at 10 nm. For urban, particle size distribution after the tailpipe was similar than the motorway cycle, with a unimodal distribution centred at 10 nm. While after the CVS, the PN size distribution was bimodal with a main mode at 50 nm and a second lower mode at 10 nm. For road, the tailpipe particle size distribution was different than motorway and urban. It showed a bimodal distribution with two main modes at 10 nm and 30 nm, and the CVS particle size distribution was unimodal and centred at 50 nm. However, a similar increase in the particle diameter and concentration was observed in the CVS as two other driving conditions. This observation could be explained by the nucleation, condensation and coagulation phenomena as described by Seinfeld (2016). The increase in particle number highlighted that nucleation process happened in the CVS. Moreover, different precursors in vehicle exhaust, such as semi volatile compounds, sulfuric acid, ammonia, polycyclic aromatic hydrocarbons (PAH), hopanes and steranes, could cause the nucleation and induce an increase in small particle numbers (Louis et al., 2016; Benson et al., 2011; Casati et al., 2007; Virtanen et al., 2006; Burtscher, 2005; Mathis et al., 2005; Zielinska et al., 2004; Bukowiecki et al., 2003). The nucleation phenomenon has already been observed in other exhaust dilution studies by Vouitsis et al. (2009) and Kittelson et al. (1998 and 2000). On the other hand, the particle growth from 10 nm to 50 nm highlighted the condensation and coagulation phenomena that depended on the SVOCs and particle concentration in the exhaust. The SVOCs condensed to the particle surface as function of the partition coefficient between the gas and the particulate phase, which induced a rapid growth of the particles (Zhang et al., 2004). The work of Albriet et al. (2010), with an aerosol computational fluid dynamics model (CFD), confirmed that SVOCs condensation governed the growth of the nanoparticles in the tailpipe plume of vehicles.

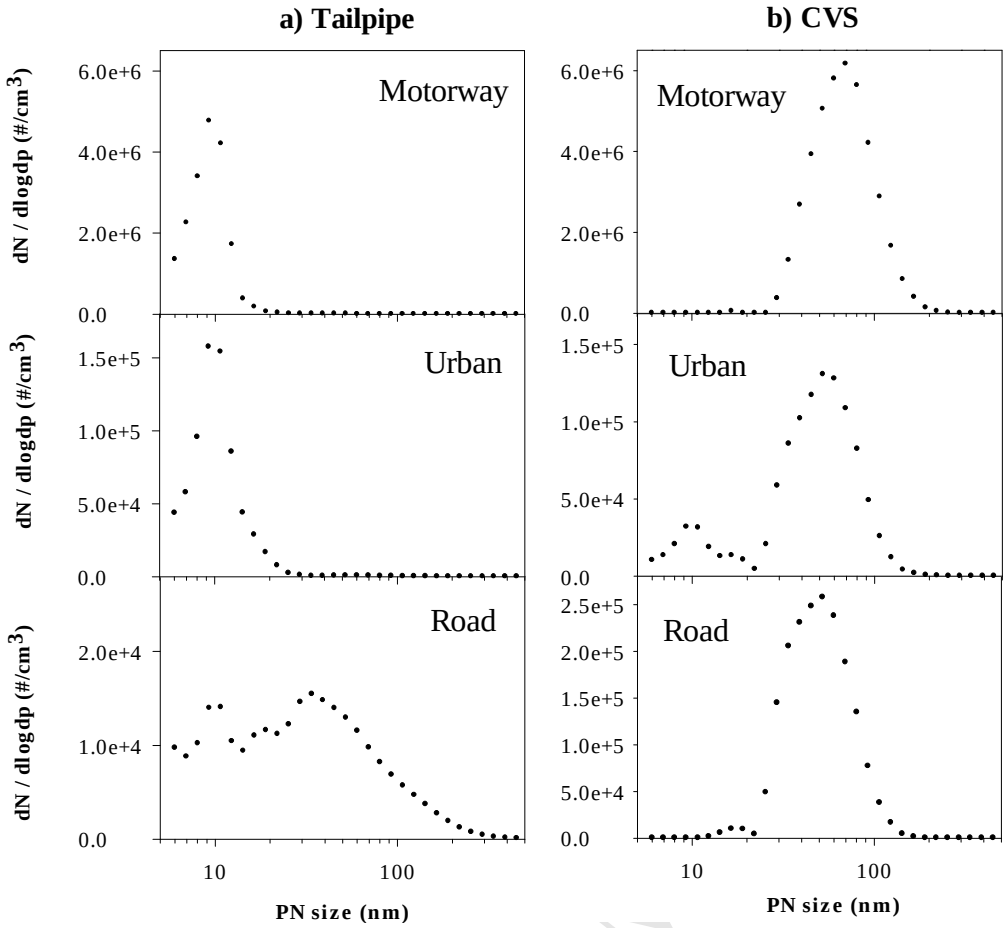

Figure 4. Euro 6 G-DI particle size distribution: a) after tailpipe and b) after CVS for Artemis motorway (at 430s), urban (at 500s) and road (at 750s). Data were measured by a Fast Mobility Particle Sizer Spectrometer (FMPS).

For urban, we also observed a particle mode at 10 nm after CVS that could be explained by the lower PN concentration and flow rate in the CVS than motorway (9 m^3/min for urban and 11 m^3/min for motorway). According to Albriet et al. (2010), turbulence remains a crucial parameter for particle growth. The CVS sampling system turbulence was calculated by the Reynolds number given by Kulkarni (2011). Reynolds number determines if the gas flow was laminar ($Re < 3\times10^3$) or turbulent ($Re > 3\times10^3$).

$$Re = \frac{U \times d}{\nu}$$

U: velocity characteristic of the gas (m/s)
d: diameter of the pipe (m)
ν: kinematic gas viscosity ($\nu = \eta/\rho_g$)

For the CVS sampling system, the Reynolds numbers were 5×10^4, 4×10^4 and 4×10^4 for the motorway, urban and road cycles respectively that were greater than the limit value (3×10^3). The CVS flow was thus a turbulent flow that promoted the phenomena of condensation and coagulation as well as the temporal diffusion of the PN concentration peaks. This turbulence was proportional to the average cycle speed. Low turbulence for the urban condition together with low PN concentration induced low coagulation and condensation rates compared to motorway condition, which could explain the bimodal PN distribution in the CVS.

316 Furthermore, high particle concentration and turbulent flow added to the Brownian motion
317 (random movement of a particle due to collisions with surrounding air particles) could induce
318 turbulent coagulation (Huang et al., 2014; Zhang et al., 2004). Table 4 (Appendix) shows an example
319 of particle coagulation time with different particle sizes and particle concentrations. The coagulation
320 coefficients used in this work were taken from Seinfeld (2016) assuming that the particles were
321 monodisperse taken into account the kinetic corrections and without turbulence. The coagulation half-
322 life time (τ_c) was determined with the following equation:

$$\tau_c = \frac{2}{K \times N_0}$$

323 K: coagulation coefficient for monodisperse aerosols;
324 N_0: particle concentration

325 For particles having mobility diameter at 10 nm, the coagulation times were 3, 100 and 1000
326 minutes (Table 4, Appendix) for the concentration at 5.5×10^6 #/cm^3, 1.6×10^5 #/cm^3 and 1.4×10^4 #/cm^3,
327 respectively, which represented motorway, urban and road PN emissions (Figure 4). For the particles
328 with diameter at 40 nm, the coagulation times were higher than 1000 minutes for all conditions.
329 According to Albriet et al. (2010) and Grieshop et al. (2009a), coagulation by diffusion is a slow
330 process that takes more than five minutes to occur, which is greater than the CVS residence time (2–10
331 seconds). The turbulence of gas flow in the sampling system could reduce the coagulation time.
332 However, coagulation is known to have a little impact on particle growth in the first seconds after the
333 exhaust (Albriet et al., 2010). These results indicated that the CVS sampling system could induce
334 nucleation and condensation phenomena influencing the particle characteristic and quantification.
335 Particle sampling at the tailpipe could represent a complementary method to better quantify the
336 particle emissions.

4 Conclusion

To investigate the effects of the exhaust dilution on particle emissions, two types of experiments were performed on a chassis dynamometer: 1) dilution and temperature effects on particle emission were investigated with Euro 5 diesel and gasoline vehicles; 2) sampling condition impacts on particle quantification were investigated with Euro 6 diesel and gasoline vehicles. The dilution and temperature effects were studied directly from tailpipe with dilution ratios ranged from 8 to 4000 and dilution temperatures from 50°C to 150°C. Low dilution temperature and low dilution ratios increased the particle number concentration by a factor of 1.4–3. The results highlighted that the low primary dilution ratios induced a significant influence on particle number concentration. At low primary dilution (3–5), the particle emission was 2 times higher than at high primary dilution (12–20). To minimise the bias, the FPS sampling system at tailpipe should be set at high primary dilution and high dilution temperature.

In the second experiment, particle emissions from tailpipe were compared to those after the CVS system under similar dilution conditions with two Euro 6 vehicles (gasoline G-DI and diesel DPFcat). Due to the high efficiency of the diesel particulate filter, PN emissions from the Euro 6 diesel vehicle were near the detection limit. For Euro 6 G-DI vehicle, CVS PN concentrations were higher than those at the tailpipe by a factor of 6, 80 and 22 for Artemis urban, road and motorway, respectively. The main particle size mode after the tailpipe was centred on 10 nm while, particle size after the CVS was centred at 70 nm for motorway and 50 nm for urban and road driving. The increase in PN concentration and the growth of particle size in the CVS were induced by the nucleation and condensation. These processes could be supported by different semi volatile particle precursors observed in our previous studies and by the turbulent flow in the sampling tunnel (Reynolds numbers = $4–5\times10^4$). The coagulation could happen in the CVS because of the high PN concentration and turbulent flow, but it remained a negligible process for the short CVS residence time (2–10s). These results indicated that the CVS sampling system could induce an over-estimation of PN. Particle sampling at tailpipe could represent a complementary method to better quantify the particle emissions.

Acknowledgements

The authors would like to thank the French Environment and Energy Management Agency (ADEME) for financial support of the CORTEA project CaPVeREA and the Auvergne Rhône-Alpes region.

References

Albriet, B., K.N. Sartelet, S. Lacour, B. Carissimo, and C. Seigneur. 'Modelling Aerosol Number Distributions from a Vehicle Exhaust with an Aerosol CFD Model'. Atmospheric Environment 44, no. 8 (March 2010): 1126–37. doi:10.1016/j.atmosenv.2009.11.025.

André, Michel. 'The ARTEMIS European Driving Cycles for Measuring Car Pollutant Emissions.' Science of The Total Environment 334–35 (December 2004): 73–84. doi:10.1016/j.scitotenv.2004.04.070.

Beckers, J., W. W. Stoffels, and G. M. W. Kroesen. 'Temperature Dependence of Nucleation and Growth of Nanoparticles in Low Pressure Ar/CH 4 RF Discharges.' Journal of Physics D: Applied Physics 42, no. 15 (2009): 155206. doi:10.1088/0022-3727/42/15/155206.

Benson, D. R., J. H. Yu, A. Markovich, and S.-H. Lee. 'Ternary Homogeneous Nucleation of H2SO4, NH3, and H2O under Conditions Relevant to the Lower Troposphere.' Atmos. Chem. Phys. 11, no. 10 (20 May 2011): 4755–66. doi:10.5194/acp-11-4755-2011.

Bukowiecki, N., J. Dommen, A. S. H. Prévôt, E. Weingartner, and U. Baltensperger. 'Fine and Ultrafine Particles in the Zürich (Switzerland) Area Measured with a Mobile Laboratory: An Assessment of the Seasonal and Regional Variation throughout a Year.' Atmos. Chem. Phys. 3, no. 5 (24 September 2003): 1477–94. doi:10.5194/acp-3-1477-2003.

Burtscher, H. 'Physical Characterization of Particulate Emissions from Diesel Engines: A Review.' Journal of Aerosol Science 36, no. 7 (July 2005): 896–932. doi:10.1016/j.jaerosci.2004.12.001.

Casati, Roberto, Volker Scheer, Rainer Vogt, and Thorsten Benter. 'Measurement of Nucleation and Soot Mode Particle Emission from a Diesel Passenger Car in Real World and Laboratory in Situ Dilution.' Atmospheric Environment 41, no. 10 (March 2007): 2125–35. doi:10.1016/j.atmosenv.2006.10.078.

Fujitani, Yuji, Katsumi Saitoh, Akihiro Fushimi, Katsuyuki Takahashi, Shuich Hasegawa, Kiyoshi Tanabe, Shinji Kobayashi, Akiko Furuyama, Seishiro Hirano, and Akinori Takami. 'Effect of Isothermal Dilution on Emission Factors of Organic Carbon and N-Alkanes in the Particle and Gas Phases of Diesel Exhaust.' Atmospheric Environment 59 (November 2012): 389–97. doi:10.1016/j.atmosenv.2012.06.010.

Giechaskiel, Barouch, Matti Maricq, Leonidas Ntziachristos, Christos Dardiotis, Xiaoliang Wang, Harald Axmann, Alexander Bergmann, and Wolfgang Schindler. 'Review of Motor Vehicle Particulate Emissions Sampling and Measurement: From Smoke and Filter Mass to Particle Number'. Journal of Aerosol Science 67 (January 2014): 48–86. doi:10.1016/j.jaerosci.2013.09.003.

Giechaskiel, B., R. Chirico, P.F. DeCarlo, M. Clairotte, T. Adam, G. Martini, M.F. Heringa, R. Richter, A.S.H. Prevot, and U. Baltensperger. 'Evaluation of the Particle Measurement Programme (PMP) Protocol to Remove the Vehicles' Exhaust Aerosol Volatile Phase.' Science of The Total Environment 408, no. 21 (1 October 2010): 5106–16. doi:10.1016/j.scitotenv.2010.07.010.

Giechaskiel, Barouch, Panagiota Dilara, and Jon Andersson. 'Particle Measurement Programme (PMP) Light-Duty Inter-Laboratory Exercise: Repeatability and Reproducibility of the Particle Number Method'. Aerosol Science and Technology 42, no. 7 (29 May 2008): 528–43. doi:10.1080/02786820802220241.

Giechaskiel, B., L. Ntziachristos, Z. Samaras, and R. Casati. 'Effect of Speed and Speed-Transition on the Formation of Nucleation Mode Particles from a Light Duty Diesel Vehicle', 2007, 15. doi:10.4271/2007-01-1110.

Grieshop, Andrew P., Marissa A. Miracolo, Neil M. Donahue, and Allen L. Robinson. 'Constraining the Volatility Distribution and Gas-Particle Partitioning of Combustion Aerosols Using Isothermal Dilution and Thermodenuder Measurements.' Environmental Science & Technology 43, no. 13 (1 July 2009): 4750–56. doi:10.1021/es8032378.

Grieshop, A. P., J. M. Logue, N. M. Donahue, and A. L. Robinson. 'Laboratory Investigation of Photochemical Oxidation of Organic Aerosol from Wood Fires 1: Measurement and Simulation of Organic Aerosol Evolution.' Atmos. Chem. Phys. 9, no. 4 (18 February 2009): 1263–77. doi:10.5194/acp-9-1263-2009.

Huang, L., S. L. Gong, M. Gordon, J. Liggio, R. Staebler, C. A. Stroud, G. Lu, C. Mihele, J. R. Brook, and C. Q. Jia. 'Aerosol–computational Fluid Dynamics Modeling of Ultrafine and Black Carbon Particle Emission, Dilution, and Growth near Roadways.' Atmos. Chem. Phys. 14, no. 23 (2 December 2014): 12631–48. doi:10.5194/acp-14-12631-2014.

Jamriska, Milan, Lidia Morawska, Steven Thomas, and Congrong He. 'Diesel Bus Emissions Measured in a Tunnel Study.' Environmental Science & Technology 38, no. 24 (1 December 2004): 6701–9. doi:10.1021/es030662z.

Karjalainen, Panu, Liisa Pirjola, Juha Heikkilä, Tero Lähde, Theodoros Tzamkiozis, Leonidas Ntziachristos, Jorma Keskinen, and Topi Rönkkö. 'Exhaust Particles of Modern Gasoline Vehicles: A Laboratory and an on-Road Study.' Atmospheric Environment 97 (November 2014): 262–70. doi:10.1016/j.atmosenv.2014.08.025.

Kim, Youngseob, Karine Sartelet, Christian Seigneur, Aurélie Charron, Jean-Luc Besombes, Jean-Luc Jaffrezo, Nicolas Marchand, and Lucie Polo. 'Effect of Measurement Protocol on Organic Aerosol Measurements

425 of Exhaust Emissions from Gasoline and Diesel Vehicles.' Atmospheric Environment 140 (September
426 2016): 176–87. doi:10.1016/j.atmosenv.2016.05.045.
427 Kittelson, David B. 'Engines and Nanoparticles : A Review.' Journal of Aerosol Science 29, no. 5/6 (1998):
428 575–88. doi:0021-8502/98.
429 Kittelson, David, Jason Johnson, and Winthrop Watts. 'Diesel Aerosol Sampling in the Atmosphere.' San Diego,
430 California, 2000. http://papers.sae.org/2000-01-2212/.
431 Köhler, Felix. 'Testing of Particulate Emissions from Positive Ignition Vehicles with Direct Fuel Injection
432 System.' Technical Report, 2013-09-26, T\HuV Nord, 2013.
433 http://www.transportenvironment.org/sites/te/files/publications/TUV-Technical_report.pdf.
434 Kozawa, Kathleen H., Arthur M. Winer, and Scott A. Fruin. 'Ultrafine Particle Size Distributions near Freeways:
435 Effects of Differing Wind Directions on Exposure.' Atmospheric Environment 63 (December 2012):
436 250–60. doi:10.1016/j.atmosenv.2012.09.045.
437 Kulkarni, Pramod, Paul A. Baron, and Klaus Willeke. Aerosol Measurement: Principles, Techniques, and
438 Applications. John Wiley & Sons, 2011.
439 Kulmala, Markku, Liisa Pirjola, and Jyrki M. Mäkelä. 'Stable Sulphate Clusters as a Source of New
440 Atmospheric Particles.' Nature 404, no. 6773 (2 March 2000): 66–69. doi:10.1038/35003550.
441 Liang, Bin, Yunshan Ge, Jianwei Tan, Xiukun Han, Liping Gao, Lijun Hao, Wentao Ye, and Peipei Dai.
442 'Comparison of PM Emissions from a Gasoline Direct Injected (GDI) Vehicle and a Port Fuel Injected
443 (PFI) Vehicle Measured by Electrical Low Pressure Impactor (ELPI) with Two Fuels: Gasoline and M15
444 Methanol Gasoline.' Journal of Aerosol Science 57 (March 2013): 22–31.
445 doi:10.1016/j.jaerosci.2012.11.008.
446 Louis, Cédric, Yao Liu, Patrick Tassel, Pascal Perret, Agnès Chaumond, and Michel André. 'PAH, BTEX,
447 Carbonyl Compound, Black-Carbon, NO2 and Ultrafine Particle Dynamometer Bench Emissions for
448 Euro 4 and Euro 5 Diesel and Gasoline Passenger Cars.' Atmospheric Environment 141 (September
449 2016): 80–95. doi:10.1016/j.atmosenv.2016.06.055.
450 Mamakos, Athanasios, and Giorgio Martini. 'Particle Number Emissions During Regeneration of DPF-Equipped
451 Light Duty Diesel Vehicles', 2011.
452 Manoukian, A., D. Buiron, B. Temime-Roussel, H. Wortham, and E. Quivet. 'Measurements of VOC/SVOC
453 Emission Factors from Burning Incenses in an Environmental Test Chamber: Influence of Temperature,
454 Relative Humidity, and Air Exchange Rate.' Environmental Science and Pollution Research 23, no. 7
455 (April 2016): 6300–6311. doi:10.1007/s11356-015-5819-2.
456 Mathis, U, M Mohr, and A Forss. 'Comprehensive Particle Characterization of Modern Gasoline and Diesel
457 Passenger Cars at Low Ambient Temperatures.' Atmospheric Environment 39, no. 1 (January 2005):
458 107–17. doi:10.1016/j.atmosenv.2004.09.029.
459 Mathis, Urs, Jyrki Ristimäki, Martin Mohr, Jorma Keskinen, Leonidas Ntziachristos, Zissis Samaras, and Pirita
460 Mikkanen. 'Sampling Conditions for the Measurement of Nucleation Mode Particles in the Exhaust of a
461 Diesel Vehicle.' Aerosol Science and Technology 38, no. 12 (January 2004): 1149–60.
462 doi:10.1080/027868290891497.
463 May, Andrew A., Albert A. Presto, Christopher J. Hennigan, Ngoc T. Nguyen, Timothy D. Gordon, and Allen L.
464 Robinson. 'Gas-Particle Partitioning of Primary Organic Aerosol Emissions: (1) Gasoline Vehicle
465 Exhaust.' Atmospheric Environment 77 (October 2013): 128–39. doi:10.1016/j.atmosenv.2013.04.060.
466 Morawska, L., Z. Ristovski, E.R. Jayaratne, D.U. Keogh, and X. Ling. 'Ambient Nano and Ultrafine Particles
467 from Motor Vehicle Emissions: Characteristics, Ambient Processing and Implications on Human
468 Exposure.' Atmospheric Environment 42, no. 35 (November 2008): 8113–38.
469 doi:10.1016/j.atmosenv.2008.07.050.
470 Ning, Zhi. 'Atmospheric Processes Influencing Aerosols Generated by Combustion and the Inference of Their
471 Impact on Public Exposure: A Review.' Aerosol and Air Quality Research, 2010.
472 doi:10.4209/aaqr.2009.05.0036.
473 Pope III, C. Arden. 'Review: Epidemiological Basis for Particulate Air Pollution Health Standards.' Aerosol
474 Science & Technology 32, no. 1 (2000): 4–14.
475 Ranjan, Manish, Albert A. Presto, Andrew A. May, and Allen L. Robinson. 'Temperature Dependence of Gas–
476 Particle Partitioning of Primary Organic Aerosol Emissions from a Small Diesel Engine.' Aerosol
477 Science and Technology 46, no. 1 (1 January 2012): 13–21. doi:10.1080/02786826.2011.602761.
478 Rönkkö, Annele Virtanen. 'Effect of Dilution Conditions and Driving Parameters on Nucleation Mode Particles
479 in Diesel Exhaust: Laboratory and on-Road Study.' Atmospheric Environment 40, no. 16 (2006): 2893–
480 2901. doi:10.1016/j.atmosenv.2006.01.002.
481 Seinfeld, John H., and Spyros N. Pandis. Atmospheric Chemistry and Physics: From Air Pollution to Climate
482 Change. John Wiley & Sons, 2016.
483 Uhrner, Ulrich, Michael Zallinger, Sibylle von Löwis, Hanna Vehkamäki, Birgit Wehner, Frank Stratmann, and
484 Alfred Wiedensohler. 'Volatile Nanoparticle Formation and Growth within a Diluting Diesel Car

Exhaust.' Journal of the Air & Waste Management Association 61, no. 4 (April 2011): 399–408. doi:10.3155/1047-3289.61.4.399.

Virtanen, A., T. Rönkkö, J. Kannosto, J. Ristimäki, J. M. Mäkelä, J. Keskinen, T. Pakkanen, R. Hillamo, L. Pirjola, and K. Hämeri. 'Winter and Summer Time Size Distributions and Densities of Traffic-Related Aerosol Particles at a Busy Highway in Helsinki.' Atmospheric Chemistry and Physics 6, no. 9 (2006): 2411–21.

Vouitsis, Elias, Leonidas Ntziachristos, Panayiotis Pistikopoulos, Zissis Samaras, Loukia Chrysikou, Constantini Samara, Chrysi Papadimitriou, Petros Samaras, and George Sakellaropoulos. 'An Investigation on the Physical, Chemical and Ecotoxicological Characteristics of Particulate Matter Emitted from Light-Duty Vehicles.' Environmental Pollution 157, no. 8–9 (August 2009): 2320–27. doi:10.1016/j.envpol.2009.03.028.

Vouitsis, Elias, Leonidas Ntziachristos, and Zissis Samaras. 'Theoretical Investigation of the Nucleation Mode Formation Downstream of Diesel after-Treatment Devices.' Aerosol and Air Quality Research 8, no. 1 (2008): 37–53.

Wang, Yan Jason, and K. Max Zhang. 'Coupled Turbulence and Aerosol Dynamics Modeling of Vehicle Exhaust Plumes Using the CTAG Model.' Atmospheric Environment 59 (November 2012): 284–93. doi:10.1016/j.atmosenv.2012.04.062.

Wei, Wenjuan, Corinne Mandin, Olivier Blanchard, Fabien Mercier, Maud Pelletier, Barbara Le Bot, Philippe Glorennec, and Olivier Ramalho. 'Temperature Dependence of the Particle/gas Partition Coefficient: An Application to Predict Indoor Gas-Phase Concentrations of Semi-Volatile Organic Compounds.' Science of The Total Environment 563–64 (1 September 2016): 506–12. doi:10.1016/j.scitotenv.2016.04.106.

Zhang, K. Max, and Anthony S. Wexler. 'Evolution of Particle Number Distribution near roadways—Part I: Analysis of Aerosol Dynamics and Its Implications for Engine Emission Measurement.' Atmospheric Environment 38, no. 38 (December 2004): 6643–53. doi:10.1016/j.atmosenv.2004.06.043.

Zhang, K.Max, Anthony S. Wexler, Yi Fang Zhu, William C. Hinds, and Constantinos Sioutas. 'Evolution of Particle Number Distribution near Roadways. Part II: The "Road-to-Ambient" Process'. Atmospheric Environment 38, no. 38 (December 2004): 6655–65. doi:10.1016/j.atmosenv.2004.06.044.

Zielinska, Barbara, John Sagebiel, Jacob D. McDonald, Kevin Whitney, and Douglas R. Lawson. 'Emission Rates and Comparative Chemical Composition from Selected in-Use Diesel and Gasoline-Fueled Vehicles.' Journal of the Air & Waste Management Association 54, no. 9 (2004): 1138–50.

516 **Appendix**

517 Table 4. CVS coagulation time for monodisperse particles as function of the PN size and
518 concentration. The coagulation coefficient takes into account the kinetic corrections but not the
519 turbulence.

Driving Cycle	PN size (nm)	PN concentration (#/cm3)	Coagulation coefficient (cm3/s)	Coagulation time (s)
Motorway	4	1.3×10^{6}	1.3×10^{-9}	1.2×10^{3}
	10	5.5×10^{6}	1.9×10^{-9}	1.9×10^{2}
	20	1.5×10^{6}	2.4×10^{-9}	5.4×10^{2}
	40	4.8×10^{3}	2.3×10^{-9}	1.8×10^{5}
	100	1.6×10^{3}	1.5×10^{-9}	8.1×10^{5}
Urban	4	4.4×10^{4}	1.3×10^{-9}	3.5×10^{4}
	10	1.6×10^{5}	1.9×10^{-9}	6.7×10^{3}
	20	1.7×10^{4}	2.4×10^{-9}	5.0×10^{4}
	40	5.2×10^{2}	2.3×10^{-9}	1.7×10^{6}
	100	2.5×10^{2}	1.5×10^{-9}	5.5×10^{6}
Road	4	9.7×10^{3}	1.3×10^{-9}	1.6×10^{5}
	10	1.4×10^{4}	1.9×10^{-9}	7.5×10^{4}
	20	1.2×10^{4}	2.4×10^{-9}	7.2×10^{4}
	40	1.5×10^{4}	2.3×10^{-9}	5.9×10^{4}
	100	5.7×10^{3}	1.5×10^{-9}	2.4×10^{5}

520

Table of Contents

Tables

Figures

Highlights

- Dilution and temperature effects on particle number emission
- Comparison between tailpipe and CVS for particle number emission
- Over-emission of particles from the CVS because of nucleation, condensation and coagulation
- Tailpipe measurement as a complementary method to the CVS for exhaust particle sampling